Biomass Conversion and Biorefinery
https://doi.org/10.1007/s13399-023-04985-1

ORIGINAL ARTICLE

Reactivity and structure: epoxidation of cottonseed oil and the corresponding fatty acid methyl ester

Yudong Meng[1,2] · **Nasreddine Kebir**[2] · **Sebastien Leveneur**[1]

Received: 15 August 2023 / Revised: 4 October 2023 / Accepted: 5 October 2023

Abstract
Vegetable oils and their functional derivatives are considered good alternatives to replace petroleum-derived products due to their low toxicity, renewability, and biodegradable properties. Due to the high viscosity of vegetable oils, the current practice is to transesterify them into fatty acid methyl esters (FAMEs) to decrease reaction mixture viscosity. The use of FAME instead of vegetable oils towards the reactivity of functionalization can have an effect. To better understand the correlation between the reactivity and structure of vegetable oils, the comparison between the epoxidation of cottonseed oil (CSO) and their corresponding fatty acid methyl ester (CSO-FAME) was carried out in this study via percarboxylic acids, produced in situ. A first comparison between the reactivity of performic and perpropionic acids was investigated. The effects of reaction temperature, HP/PA ratio, and catalyst loading on the epoxidation of CSO and CSO-FAME were evaluated. Important analytical work was done by using FTIR, NMR, GPC, and titrations to track the reaction extent and the nature of ring-opening products. The results show that CSO-FAME has a faster reaction rate both in epoxidation and ring-opening reactions. The use of perpropionic acid decreases the side reaction of ring-opening. The kinetics of CSO epoxidation was found to be faster than CSO-FAME.

Keywords Cottonseed oil · Epoxidation · Fatty acids methyl ester · Kinetic · Structure reactivity

1 Introduction

Using renewable raw materials, such as biomass, to substitute non-renewable resources is attracting more researchers' interest in chemical industries [1]. Valorizing biomass is a crucial way to address global warming problems and the depletion of fossil feedstocks [2, 3].

The example of vegetable oil valorization for biodiesel production shows its importance in academic and industrial research [2, 4]. After chemical modifications, some products and intermediates could be obtained from vegetable oils, such as polymers, emulsions, lubricants, coatings, and gels [5]. Vegetable oils and their functional derivatives can be considered good alternatives to replace petroleum-derived products due to their low toxicity, renewability, and biodegradable properties [6–8]. One of the best approaches to functionalize vegetable oils is the epoxidation of the unsaturated groups [9]. Epoxidation is generally used in the chemical industries to manufacture environment-friendly plasticizers and stabilizers for polymers, precursors, or intermediates for non-isocyanate polyurethanes [10].

The Prileschajew approach is the most common method to generate epoxidized vegetable oil using in situ–produced percarboxylic acids [11, 12]. The generated percarboxylic acids, acting as oxygen carriers, permeate in the unsaturated parts of the organic phase to progress the epoxidation [13, 14]. In the organic phase, the solubility of hydrogen peroxide is relatively low, so the Prileschajew method is quite popular and usually accompanied by an acid catalyst to accelerate the velocity of the perhydrolysis reaction step [15]. However, this reaction system has two main drawbacks: side reactions of ring opening and the thermal issue linked to exothermic reaction steps [16]. It is shown that the percarboxylic acid is not thermally stable [17]. The ring-opening reaction is influenced by protons

✉ Sebastien Leveneur
sebastien.leveneur@insa-rouen.fr

[1] NSA Rouen Normandie, UNIROUEN, Normandie Univ, LSPC, UR4704, F-76000 Rouen, France

[2] Laboratoire PBS, INSA Rouen Normandie, UNIROUEN, Normandie Université, UMR CNRS 6270 & FR 3038, Avenue de l'Université, 76801 Saint Etienne du Rouvray, France

Published online: 17 October 2023

from carboxylic acids and homogeneous catalyst dissociation [18, 19]. The use of solid acid can circumvent the negative effect of homogeneous catalysts because the internal catalyst site is less accessible for epoxidized vegetable oils but not for carboxylic acids. Additionally, a longer chain percarboxylic acid is less acidic than the shorter ones, such as formic or acetic acids, which are the most used for this reaction. According to some articles, ring-opening reactions lead to the production of diol or similar products [20, 21].

The first step is to transesterify vegetable oil into fatty acid methyl ester (FAME) to ease the valorization of vegetable oils. Transesterification of triglycerides by methanol is done by acid, base, or enzyme catalysis or under supercritical conditions [22, 23]. The viscosity of fatty acid methyl ester is lower than their corresponding vegetable oil, allowing an easier and better mixing of the reaction mixture [24, 25]. The transesterification of vegetable oils into FAMEs could decrease steric hindrance during epoxidation [26, 27].

Formic and acetic acids, the most generally employed carboxylic acids in epoxidation, are very reactive but are strong acids favoring ring-opening reactions [28]. To overcome the negative effects of those two carboxylic acids, the epoxidation reaction of cottonseed oil by perpropionic acid over a solid acid catalyst was investigated. Comparing to acetic and formic acid, propionic acid is less acidic and more stable [29]. Previous studies demonstrated that the catalyst Amberlite IR-120 accelerates the generation rate of the percarboxylic acid through perhydrolysis [30]. Hence, propionic acid and Amberlite IR-120 could decrease the ring-opening reaction compared to homogeneous and formic acid catalysts. The kinetics of epoxidation via performic and perpropionic acid over Amberlite IR-120 was carried out to confirm this assumption.

As mentioned previously, the transesterification of vegetable oils into FAMEs decreases the viscosity, but few studies compare the kinetics of epoxidation of vegetable oils and its corresponding FAMEs over solid catalysts. Hence, a systematic comparison between the reactivity of epoxidation of CSO and CSO-FAME was done in this manuscript. A profound analytical investigation was carried out via FTIR, NMR, and GPC. The effects of reaction temperature, HP/PA ratio, and catalyst loading on the epoxidation reaction of CSO and CSO-FAME were investigated to understand the reactivity difference and propose a reaction mechanism.

2 Materials and methods

2.1 Materials and chemical

Cottonseed oil, propionic acid, formic acid, potassium iodide, and sodium thiosulfate solution (0.1 mol/L) were purchased from Thermo Fisher Scientific (Schwerte, Germany). Hydrogen peroxide (33 wt% in water), tetraethylammonium bromide (TEAB), and perchloric acid (0.1 mol/L in acetic acid) were purchased from VWR International (Fontenay-sous-Bois, France). Magnesium sulfate, chloroform, methanol, iodine solution (0.1 mol/L), sodium thiosulfate solution (0.1 mol/L), and Amberlite IR-120 were obtained from Sigma-Aldrich (Burlington, USA).

2.2 Reactions

2.2.1 Esterification reaction

The esterification reactions were operated in a 300-mL glass-jacketed reactor. Esterification of CSO was performed by the mean of Campanella et al. with a slight modification [31]. In the present system, preheated 50 mL of methanol with 2.1 g NaOH was added to 200 g preheated cottonseed oil in the reactor, and the esterification was kept for 1.5 h. The glycerol layer was removed after the mixture was stratified into two phases. Then, the rest of the separated methyl ester layer in the reactor was cleaned three times with 600 mL of distilled water with one drop of H_3PO_4. The methyl ester layer was collected after being cleaned 3 times by distilled water and evaporated by an IKA RV10 control vacuum rotary evaporator (VWR, Darmstadt, Germany) at 65 °C for 2 h and dried by $MgSO_4$. The final product of CSO-FAME was kept at 4 °C.

2.2.2 Epoxidation reaction

The epoxidation reactions were operated in a 300-mL glass-jacketed reactor containing mechanical stirring, temperature probes, and a reflux condenser. In the present system, a mixture of the organic phase (CSO or CSO-FAME), catalyst (Amberlite IR-120), and aqueous phase (33 wt% hydrogen peroxide and distilled water) was added in the reactor to be preheated. The rotating speed was fixed at 600 rpm, where no mass transfer resistance was observed. Then, the preheated propionic acid (or formic acid) solution was added to the reactor when the mixture reached the desired temperature. During the epoxidation, a syringe collected samples in a 10-mL centrifugal tube over time. Then, the layers of organic and aqueous were isolated by a Rotofix 32A centrifuge (Hettich, Tuttlingen, Germany) at 6000 rpm/min for 4 min. Both parts were analyzed and kept at 4 °C. The mixture was stratified into two phases at the end of the epoxidation reaction, and the aqueous phase was removed. Then, the organic phase was cleaned with distilled water for 3 times and evaporated by an IKA RV10 control vacuum rotary evaporator (VWR, Darmstadt, Germany) at 65 °C for 2 h. The final product (ECSO or ECSO-FAME) was kept at 4 °C.

The experimental matrix for the study of CSO and CSO-FAME epoxidation via performic or perpropionic acids are displayed in Table 1.

Experimental runs for CSO and CSO-FAME epoxidation kinetics by perpropionic acid are displayed in Tables 2 and 3.

2.3 Analytical methods

2.3.1 NMR analysis

MSL-300 NMR spectrometer (Bruker Corporation, Billerica, USA) was employed to conduct the ^{1}H NMR analysis at 300 MHz in $CDCl_3$ solutions with a TMS (tetramethylsilane) internal standard.

2.3.2 FTIR analysis

Spectrum 2000 FTIR (PerkinElmer, Inc., Waltham, Massachusetts, USA) with a diamond ATR device was employed to conduct the FTIR analysis and spectra were obtained from 10 scans in the range of 650 to 4000 cm^{-1}.

2.3.3 GPC analysis

Average molecular weights (Mn and Mw) and dispersity ($Đ$ = Mw/Mn) were investigated by size exclusion chromatography (SEC). Samples were dissolved in dichloromethane and filtered (0.45 µm). Then, Varian PL-GPC50 system (Agilent Technologies, Santa Clara, California, USA) with two mixed packed columns (PL gel mixed type C) was applied for the analysis. The system used dichloromethane as the mobile phase and PMMA standards (from 875 to 62000 g mol^{-1}) for calibration.

2.3.4 Double bond content

The concentration of double bond was calculated by iodine value and measured by Wijs approach [32]. Briefly, 0.20 g of sample was dissolved in 20 mL of chloroform. Then, 25 mL of Wijs solution (0.1 mol/L) was added. After 1 h in the dark, 20 mL of 10% KI solution was added. After

Table 1 Experimental runs for the kinetics of epoxidation of CSO

CSO	T (K)	Initial mass (g)					Initial concentration (mol/L)				
		Catalyst	Oil	Acid	33% HP	H_2O	$[H_2O]_{aq}$	$[DB]_{org}$	$[Ep]_{org}$	$[HP]_{aq}$	$[CA]_{aq}$
FA	303.15	5.0	100.00	46.00	83.00	71.00	35.17	3.91	0.00	4.03	5.00
PA	303.15	5.0	100.00	74.00	83.00	43.00	27.39	3.91	0.00	4.03	5.00
CSO-FAME	T (K)	Catalyst	Oil	Acid	33% HP	H_2O	$[H_2O]_{aq}$	$[DB]_{org}$	$[Ep]_{org}$	$[HP]_{aq}$	$[CA]_{aq}$
FA	303.15	5.00	100.00	46.00	83.00	71.00	35.17	4.02	0.03	4.03	5.00
PA	303.15	5.00	100.00	74.00	83.00	43.00	27.39	4.02	0.03	4.03	5.00

Table 2 Experimental runs for the kinetics of epoxidation of CSO

RUN	T (K)	Initial mass (g)					Initial concentration (mol/L)				
		Catalyst	CSO	33% HP	PA	H_2O	$[H_2O]_{aq}$	$[DB]_{org}$	$[Ep]_{org}$	$[HP]_{aq}$	$[PA]_{aq}$
0	330.88	0.0	100.00	83.00	74.00	43.00	27.51	3.85	0.00	4.03	4.99
1	341.05	10.2	100.10	85.30	73.00	42.10	27.51	3.85	0.03	4.13	4.92
2	331.84	9.8	100.10	84.50	74.00	44.00	27.60	3.85	0.03	4.05	4.93
3	323.15	10.0	100.10	86.30	73.30	42.90	27.63	3.85	0.03	4.14	4.89
4	333.15	5.0	100.00	83.00	74.00	43.00	27.39	3.85	0.03	4.03	4.99
5	333.15	10.0	100.00	144.60	44.50	11.00	29.95	3.85	0.03	7.01	3.00
6	333.15	10.0	100.00	61.80	103.71	34.35	21.06	3.85	0.03	3.00	7.00

Table 3 Experimental runs for the kinetics of epoxidation of CSO-FAME

RUN	T (K)	Initial mass (g)					Initial concentration (mol/L)				
		CAT	FAME	33% HP	PA	H_2O	$[H_2O]_{aq}$	$[DB]_{org}$	$[Ep]_{org}$	$[HP]_{aq}$	$[PA]_{aq}$
0	330.88	0.0	100.00	83.00	74.00	43.00	27.51	3.91	0.00	4.03	4.99
1	341.05	10.2	100.10	85.30	73.00	42.10	27.51	3.91	0.03	4.13	4.92
2	331.84	9.8	100.10	84.50	74.00	44.00	27.60	3.91	0.03	4.05	4.93
3	323.15	10.0	100.10	86.30	73.30	42.90	27.63	3.91	0.03	4.14	4.89
4	333.15	5.0	100.00	83.00	74.00	43.00	27.39	3.91	0.03	4.03	4.99
5	333.15	10.0	100.00	144.60	44.50	11.00	29.95	3.91	0.03	7.01	3.00
6	333.15	10.0	100.00	61.80	103.71	34.35	21.06	3.91	0.03	3.00	7.00

adding 100 mL water, the concentration of double bond was titrated by standard $Na_2S_2O_3$ solution (0.1 mol/L) with an automatic titrator (916 Ti-Touch, Metrohm, Herisau, Switzerland) and calculated by the following formula:

$$[DB] = \frac{\left(V_{\text{blank}} - V_{\text{titration}}\right) \times c_{\text{sodium thiosulphate}}}{\left(\frac{m_{\text{sample}}}{\rho_{\text{sample}}}\right) \times 2}$$

2.3.5 Epoxide content

The approach of Maerker was applied to measure the concentration of epoxide group [33]. Briefly, 0.10 g of sample was dissolved in 10 mL of chloroform. Then, 10 mL of TEAB solution (20% TEAB in acetic acid) was added. The concentration of epoxidized group was titrated by standard perchloric acid in acetic acid solution (0.1 mol/L) with an automatic titrator (916 Ti-Touch, Metrohm) and calculated by the following formula:

$$[EP] = \frac{V_{\text{titration}} \times c_{\text{perchloric acid}}}{\left(\frac{m_{\text{sample}}}{\rho_{\text{sample}}}\right)}$$

2.3.6 Ring-opening products

The concentration of ring-opening products (ROPs) was estimated from the knowledge of the initial concentration of double bond $[DB]_0$; the concentration of double bond at time t, $[DB]_t$; and epoxide at time t, $[EP]_t$. At initial time, the concentration of epoxide is zero. Thus, the concentration of ring-opening products can be calculated as:

$$[ROP]_t = [DB]_0 - [DB]_t - [EP]_t$$

2.3.7 Calculation of conversion, selectivity, and yield

The conversion of double bond was calculated using the following equation:

$$Conversion_{DB} = \frac{[DB]_0 - [DB]}{[DB]_0} \times 100\%$$

where $[DB]_0$ is the initial concentration of double bond and [DB] is the final concentration of double bond.

The selectivity of epoxide group was calculated using the following equation:

$$Selectivity_{EP} = \frac{[EP]}{[DB]_0 - [DB]} \times 100\%$$

where $[DB]_0$ is the initial concentration of double bond, [DB] is the final concentration of double bond, and [EP] is the final concentration of epoxide group.

The yield of epoxide group was calculated using the following equation:

$$Yield_{EP} = \frac{[EP]}{[DB]_0} \times 100\%$$

where $[DB]_0$ is the initial concentration of double bond and [EP] is the final concentration of epoxide group.

3 Results and discussion

The reaction stage of esterification and epoxidation reactions are shown in Fig. 1. CSO-FAME was obtained by transesterifying CSO with methanol catalyzed by sodium hydroxide. The epoxidation of CSO and CSO-FAME using a combination of hydrogen peroxide and carboxylic acid is a biphasic liquid-liquid system. All concentrations were measured three times, and the uncertainty evaluated with standard deviations was less than 0.05 mol/L.

3.1 Characterization of the native and modified CSO products

The spectroscopy methods including NMR, FTIR, and GPC were applied further to identify the organic phase after esterification and epoxidation reaction and get more information about side reactions of polymerization and ring-opening reactions.

3.1.1 FTIR analysis

The FTIR spectra of CSO (cottonseed oil), CSO-FAME (cottonseed oil fatty acid methyl ester), epoxidized cottonseed oil (ECSO), and epoxidized cottonseed oil fatty acid methyl ester (ECSO-FAME) are displayed in Fig. 2. For wavenumber higher than 1500 cm^{-1}, peaks from FAME and CSO were the same. From 1700 to 1800 cm^{-1}, the detected peaks can be ascribed to the stretching vibration of C=O, representative of esters found in both CSO and CSO-FAME. The band at around 3000 cm^{-1} corresponds to the bond stretching between hydrogen and a sp2 carbon (=C–H). Figure 2 also shows that this carbon-carbon double bond remains stable after the esterification reaction of CSO, leading to CSO-FAME. The main spectrum region to discriminate the chemical compositions between CSO and CSO-FAME is in the range of 900–1500 cm^{-1}. The band at around 1450 cm^{-1}, absent in CSO, is ascribed to the asymmetric stretching of $–CH_3$, in the methyl ester group. The band at about 1200 cm^{-1} corresponds to O–CH3 stretching in the methyl ester group.

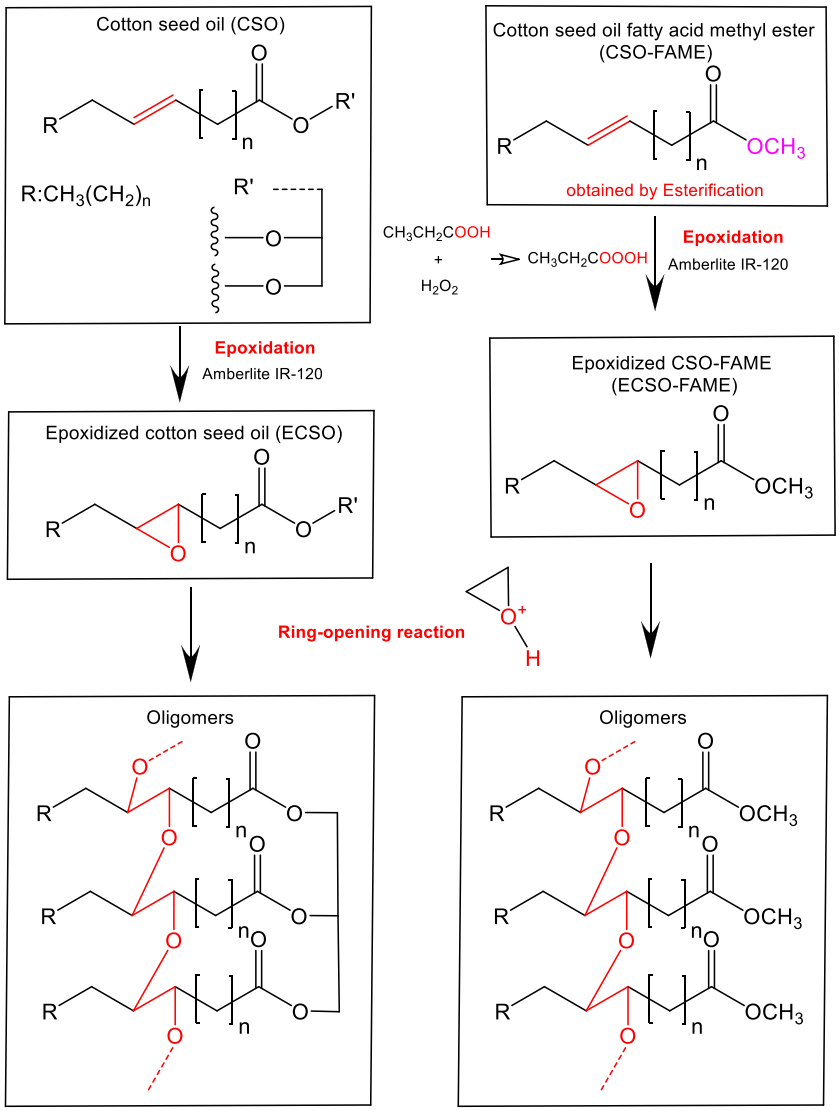

Fig. 1 Reaction stages of esterification and epoxidation

After the epoxidation reaction, the conversion of the double bond (CH=CH) into oxirane in CSO and CSO-FAME could be characterized by the disappearance of the corresponding band around 3000–3050 cm^{-1} and the appearance of a band of the epoxidized group at about 850 cm^{-1} [34].

3.1.2 NMR analysis

NMR spectra of CSO, CSO-FAME, ECSO, and ECSO-FAME are displayed in Fig. 3. According to Fig. 3, the methyl ester group (3.7 ppm) can be clearly observed in the CSO-FAME spectrum without the signal at 4.2 ppm ascribed to the CH_2 groups in the glyceridic part after the esterification reaction. One can also observe a decrease in the peak at around 5.2 ppm owing to the disappearance of the CH proton peak, which overlaps with the peak of the olefinic protons (Figures S1-S4) [35].

After the epoxidation reaction of CSO and CSO-FAME, one can observe the disappearance of the peak of the double bond (around 5.2 ppm), which was converted into a peak of the epoxidized group (around 3.0 ppm). The methyl ester group can also be observed in the ECSO-FAME spectrum with the absence of four glyceridic proton signal at 4.2 ppm. The lack of signals between 3.6 and 3.8 ppm in the ^1H NMR spectra implies the absence of hydroxyl groups coming from hydrolytic degradation of the triglyceride in ECSO (absence of free glycerol or semi-hydrolyzed ECSO) which is verified by the integrations of the peaks of the protons in the alpha position to the oxygen of the ester groups, compared to the integration of the methyl peaks (Figures S1-S4) [36]. The absence of these signals also means the absence of hydroxyl group coming from hydrolytic epoxide ring opening in both ECSO and ECSO-FAME. However, this does not mean that the ring opening favored by water and providing diols (as

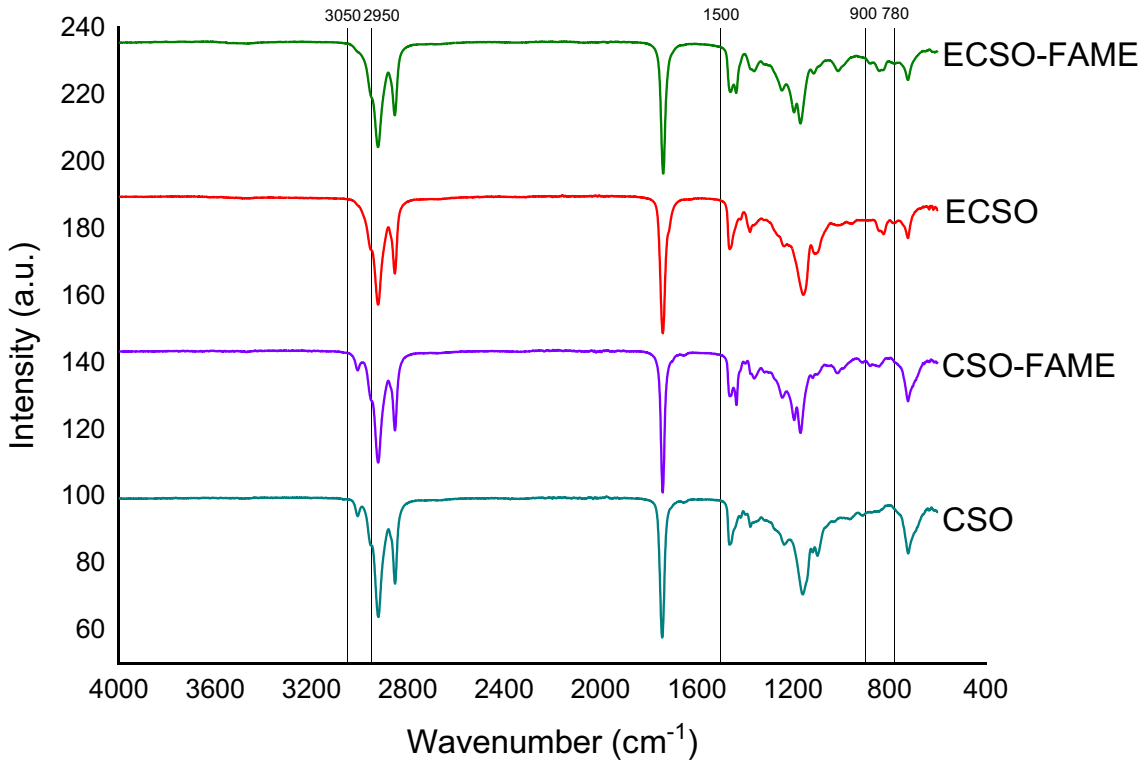

Fig. 2 FTIR spectra for the CSO, CSO-FAME, ECSO, and ECSO-FAME

observed in the literature) does not take place, but that any diols that might be formed transiently would be immediately eliminated under our operating conditions by producing new carbon-carbon double bonds, which would be epoxied again.

3.1.3 GPC analysis

GPC results of CSO, CSO-FAME, ECSO, and ECSO-FAME are displayed in Fig. 4. In the GPC chromatogram of CSO, a narrow main peak could be observed corresponding to the triglyceride molecule. It can also be observed that a minor peak of higher molecular weight corresponds to a siccative minority portion of the triglyceride molecule. As expected, since the CSO-FAME resulted from the CSO cleavage by transesterification, it exhibited a lower molecular weight. Moreover, the glycerol was removed.

After the epoxidation, GPC chromatograms of ECSO and ECSO-FAME show a shift of the main peak to a higher molecular weight region, implying that the ring-opening/elimination side-products are in a low extent. A secondary peak that can also be observed in both ECSO and ECSO-FAME are ascribed to oligomers resulting from ring-opening/cationic polymerization reactions [37]. The oligomer production from ECSO and ECSO-FAME is similar, but the three-armed star structure of ECSO could allow a higher availability of access to the unsaturated groups.

The third population in ECSO-FAME starting from the right is the saturated CSO-FAME chains that cannot be modified by epoxidation and cannot go through an increase in molecular weight. In the CSO, saturated and unsaturated chains cannot be discriminated in the GPC spectra since they are attached to the same molecule (triglyceride). Indeed, the epoxidation of only one double bond in one of the three chains of the triglyceride molecule led to an increase in the average molecular weight. In addition, ECSO also presents an oligomerized part.

3.2 Comparison of the epoxidation kinetics between formic and propionic acids

The impact of carbon chain length from carboxylic acid on the CSO and CSO-FAME's epoxidation was carried out using formic and propionic acids (Table 1 and Fig. 5).

These experiments were performed at 30 °C to avoid high energy released in the case of formic acid, making difficult to maintain isothermal conditions. All these experiments were performed with the same initial concentrations and catalyst loading.

Figure 5 shows that the epoxidation rate using formic acid is faster than experiments carried out with propionic acid. At this reaction temperature, the epoxidation rate is slightly faster for CSO-FAME than CSO with formic, but this rate is

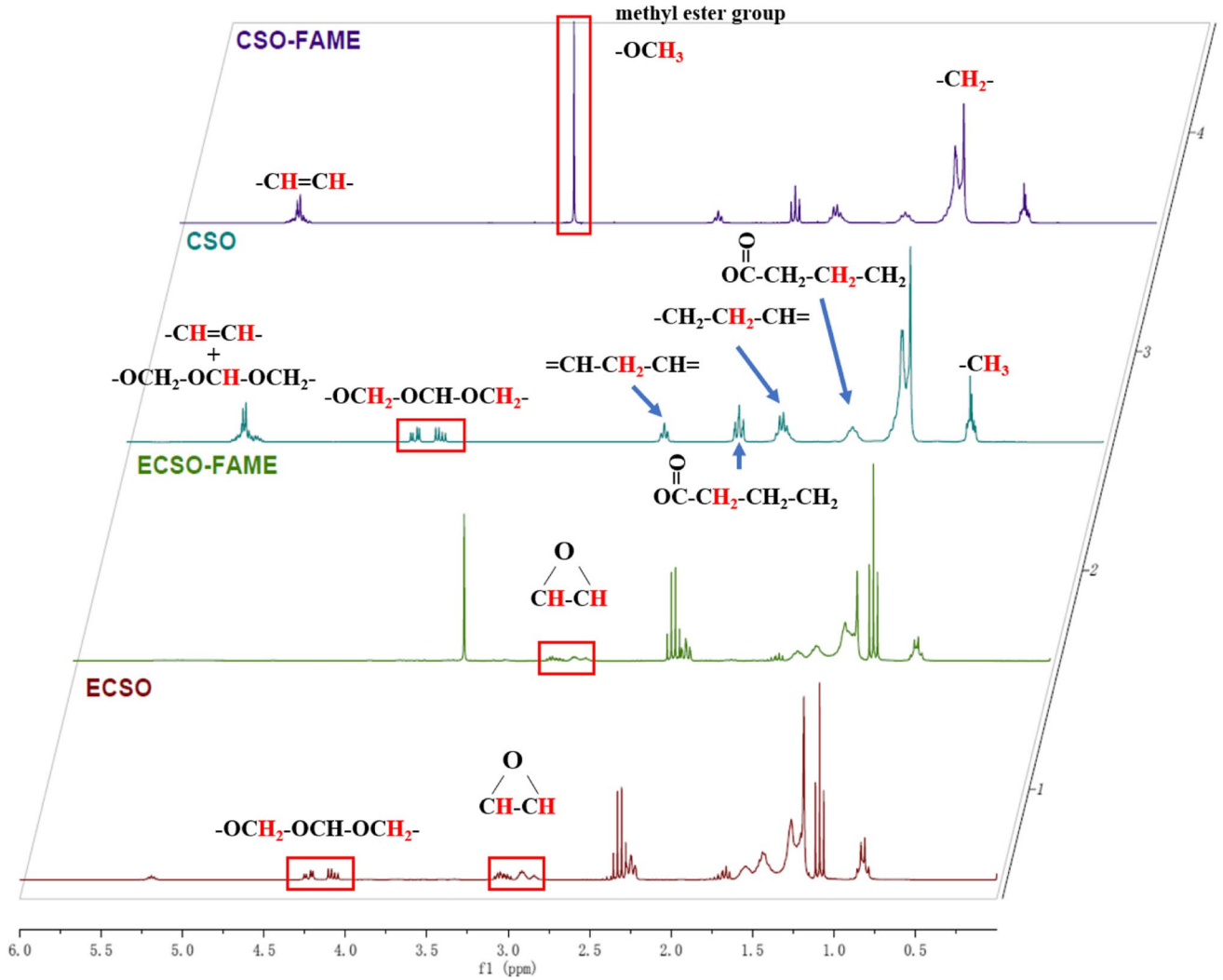

Fig. 3 ^{1}H NMR spectra for CSO, CSO-FAME, ECSO, and ECSO-FAME

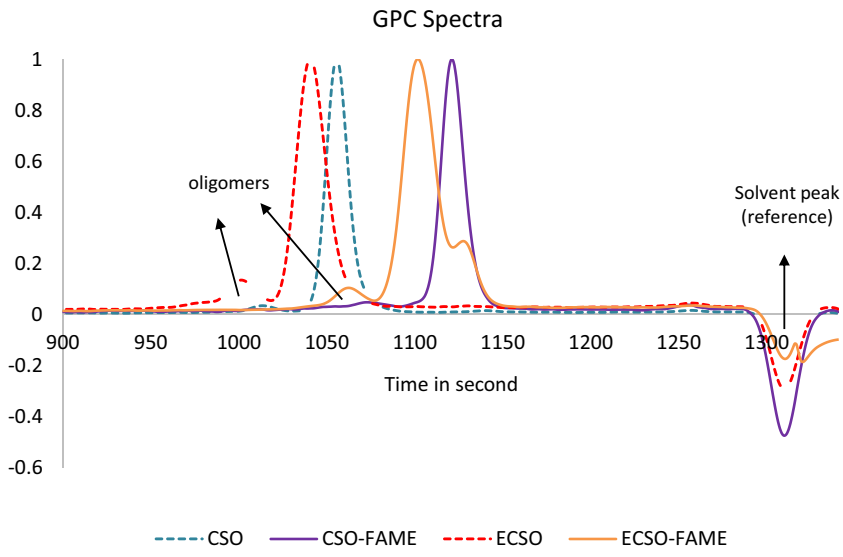

Fig. 4 GPC spectra for CSO, CSO-FAME, ECSO and ECSO-FAME

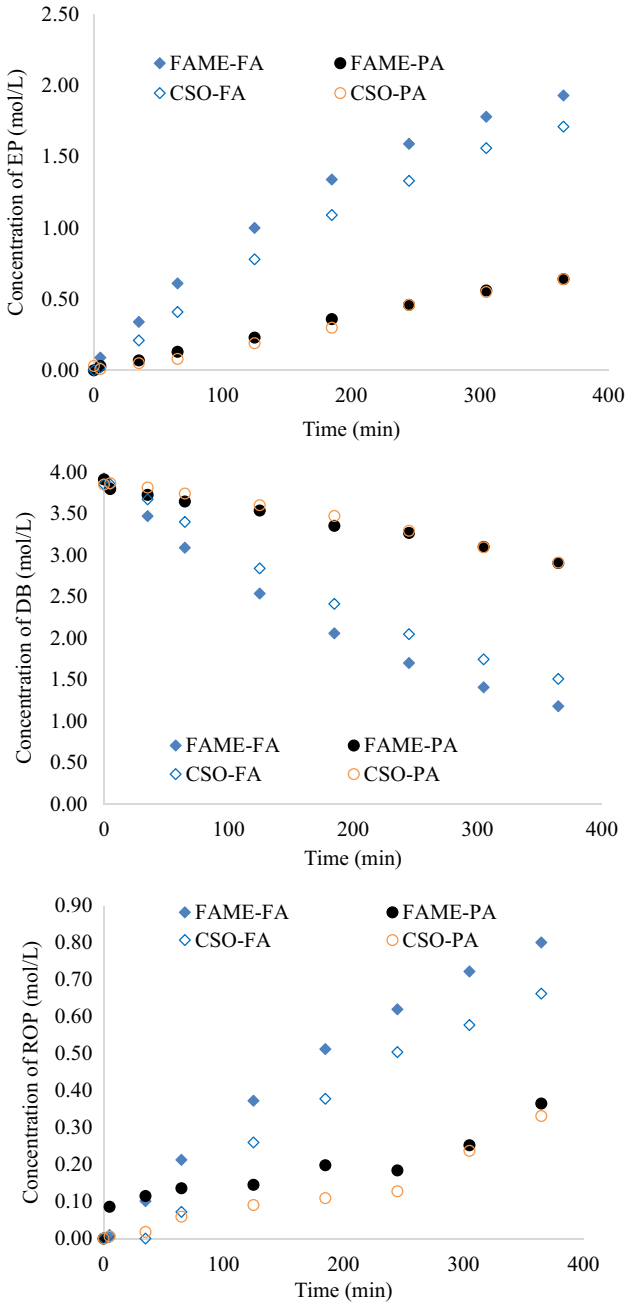

Fig. 5 Effects of different acids on the epoxidation of CSO and CSO-FAME (FA, formic acid; PA, propionic acid)

similar for CSO-FAME and CSO with propionic acid. The same observation can be done for the rate of double bond consumption.

However, Fig. 5 shows that the rate of ring-opening products is more significant for formic acid. The ring-opening product was 0.8 mol/L after 365 min of reaction, with the concentration of epoxide groups 1.9 mol/L for the formic acid experiment. Using formic acid speeds up the kinetics of epoxidation and the kinetics of ring-opening and decomposition of performic acid. Thus, with a higher temperature or longer reaction time, more ring-opening reactions will lead to a lower concentration of epoxidized group for experiments carried out with formic acid. Therefore, with the presence of Amberlite, propionic acid could produce epoxidized vegetable oils and their fatty acids methyl esters with a higher concentration of oxirane.

From this study, the use of propionic acid is better from a selectivity standpoint.

3.3 Comparison of the epoxidation kinetics between CSO and CSO-FAME

For the kinetic study, titration measurements were applied to track concentrations of the double bond and epoxidized groups at different operating conditions (Tables 2 and 3). Conversion, selectivity and yield of each run for CSO and CSO-FAME are displayed in Table S1, and the repeatability of the epoxidation with propionic acid is shown in Figure S5.

3.3.1 Study of the effect of reaction temperature

As displayed in Fig. 6 (runs 1, 2, and 3 in Tables 2 and 3), the reaction rates of epoxidation for CSO and CSO-FAME increase with the temperature from 50 to 70 °C. The ring-opening reaction can be observed from the concentration of DB and EP at the end of the epoxidation kinetic profiles, which are lower than the initial concentration of the double bond. From Fig. 6, the production rate of epoxidized group is faster for CSO than for CSO-FAME, and the final production of epoxidized group is higher for CSO than for CSO-FAME. This observation is *a priori* surprising because one could expect that the double bond from CSO-FAME is more accessible than the one from CSO, and thus, rates of double bond epoxide production should be faster. This reactivity difference towards epoxidized groups is more pronounced when the reaction temperature increases. The rate of double bond consumption is faster for CSO than for CSO-FAME. This kinetic observation could be explained by the fact that the ring-opening reactions and consecutive oligomerization reactions produce different oligomer structures between ECSO and ECSO-FAME. Due to ring-opening, the oligomerization for ECSO-FAME produces linear oligomer, making less accessible the double bond with reaction progress from a steric standpoint (Fig. 4).

3.3.2 Study on the effect of HP/PA ratio

The kinetics of epoxidation is influenced by the kinetics of perhydrolysis and, thus, by the ratio HP/PA. The effects of the HP/PA ratio on the rate of epoxidation reaction of

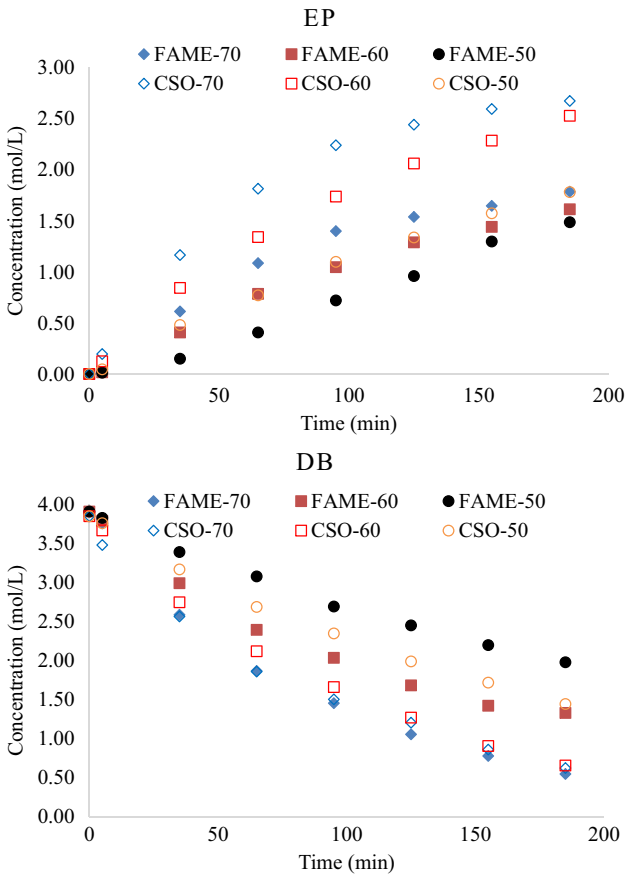

Fig. 6 Effects of reaction temperature on the epoxidation of CSO and CSO-FAME by perpropionic acid (runs 1, 2, and 3 from Tables 2 and 3)

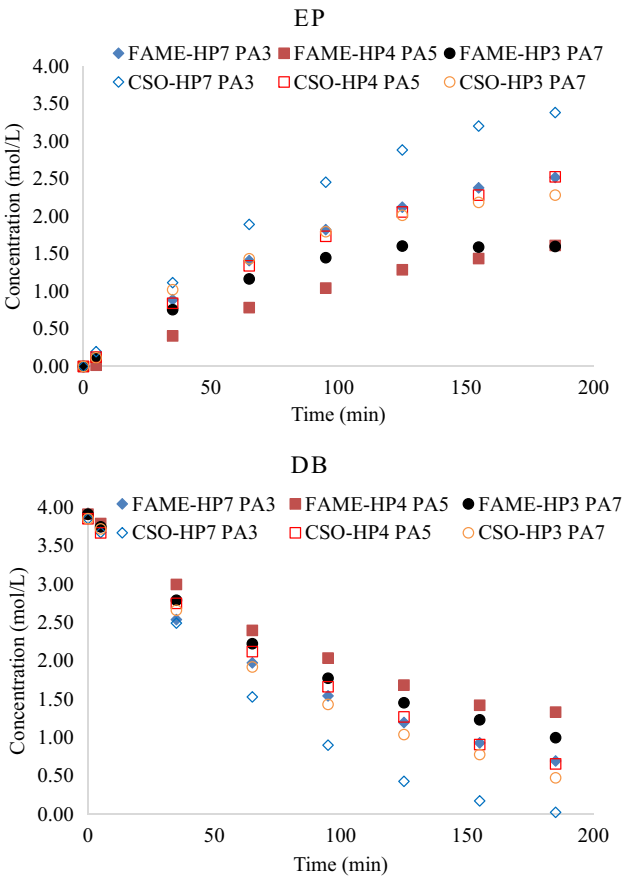

Fig. 7 Effects of HP/PA ratio on the epoxidation of CSO and CSO-FAME by perpropionic acid (runs 2, 5, and 6 in Tables 2 and 3)

CSO and CSO-FAME are shown in Fig. 7 (runs 2, 5, and 6 in Tables 2 and 3). When the ratio HP/PA is equal to 7/3, the reaction rate of epoxidation is higher, producing more oxirane groups. In contrast, at an HP/PA ratio equal to 3/7, the reaction rate of epoxidation is slower. This observation could be linked to the fact that at a low HP/PA ratio, the kinetics of perpropionic acid in the aqueous phase is slower, explaining the similar initial reaction rates of DB consumption. At any HP/PA ratio, rates of epoxide production are faster for CSO than for CSO-FAME. A higher HP/PA ratio increases the epoxidation rate and improves the epoxidized group's conversion yield. This could be explained that the higher concentration of PA increase proton concentration, catalyzing the ring-opening reaction.

3.3.3 Study on the effect of catalyst loading

The effects of the catalyst loading on CSO and CSO-FAME are displayed in Fig. 8. For the catalyst, Amberlite IR-120 was employed to catalyze the perhydrolysis, in other words, the generation rate of perpropionic acid. Compared to the catalyst loading of 0 g, 5 g, and 10 g (runs 0, 2, and 4 in Tables 2 and 3), the epoxidation rate decreases with less catalyst loading. It could be noticed that there were no differences in the epoxidation rates between CSO and CSO-FAME without catalysts, showing the importance of perhydrolysis reaction on the kinetics of epoxidation. More catalyst loading speeds up the perhydrolysis rate and produces more perpropionic acid, increasing the epoxidation rate. At the same catalyst loading (higher than 0 g), epoxidation of CSO is faster than FAME.

3.4 Comparison of the side-reaction between CSO and CSO-FAME

In the epoxidation reaction, the double bonds are epoxidized by the perpropionic acid. However, the oligomer group produced from the polymerization could play a vital role on the selectivity towards oxirane groups.

By the previous discussion, some oxirane undergo ring-opening reactions leading to ring-opening products (ROP). Comparing the side reaction between CSO and CSO-FAME could give a better insight into explaining the difference of reactivity between CSO and FAME.

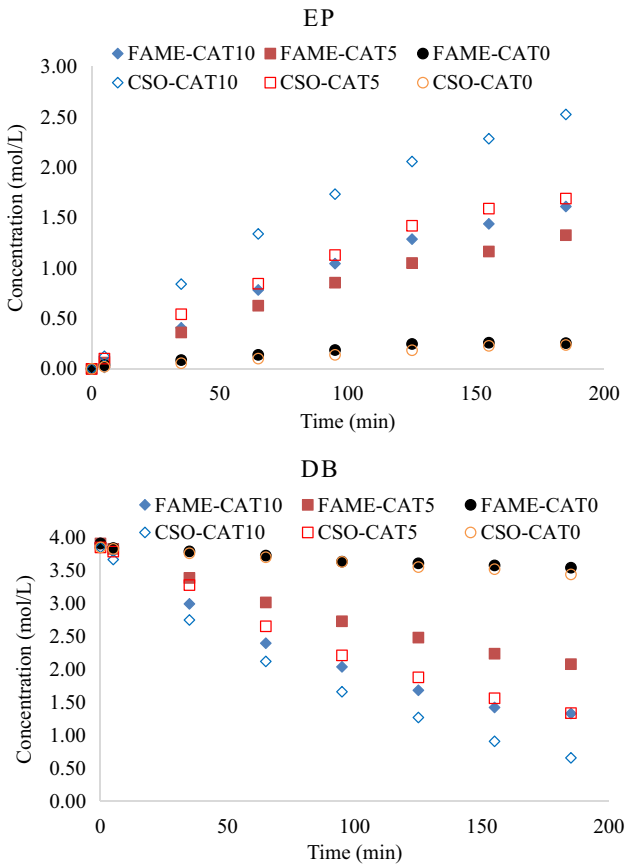

Fig. 8 Effects of catalyst loading on the CSO and CSO-FAME

3.4.1 Study on the effect of reaction temperature

As shown in Fig. 9, the rate of ring-opening products (ROPs) is affected by temperatures and increases with temperature. However, the reaction rate of ring-opening production is faster for CSO-FAME compared to CSO. After 185-min epoxidation at 70 °C, the concentrations of ROP was higher for ECSO-FAME than CSO system. Figure 9 shows that side ring-opening reactions are more pronounced for ECSO-FAME system than CSO system.

3.4.2 Study on the effect of HP/PA ratio

As shown in Fig. 10, a higher HP/PA ratio leads to a lower reaction rate of the side reaction. It could also be noticed that the ring-opening reactions was also influenced by HP/PA ratio, but CSO-FAME still has a higher reaction rate in the side reaction than CSO. Therefore, a higher HP/PA ratio enhances epoxidation and restrains the side reactions to ensure selectivity towards oxirane.

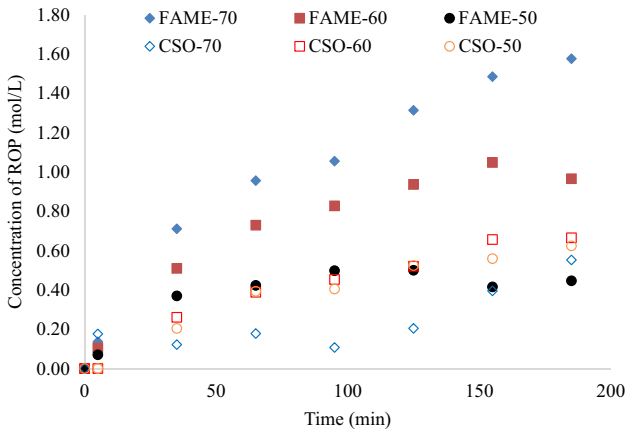

Fig. 9 Effects of reaction temperature on the ring-opening products

3.4.3 Study on the effect of catalyst loading

The effect of the catalyst loading on the side-reaction rate is displayed in Fig. 11. CSO-FAME usually has a higher level of ring-opening reactions than CSO if they have the same conditions of temperature, HP/PA ratio, and catalyst loading. Nevertheless, the side reaction rate is similar, with no catalyst in the reaction system. The situation changed if adding catalyst to accelerate the perhydrolysis of propionic acid. One interesting observation is that the side-reaction rate of CSO and CSO-FAME increased with the increase of catalyst loading, but more ring-opening products could be found in CSO at catalyst loading of 5 g and more in CSO-FAME when the catalyst loading is 10 g. The ring-opening products of CSO at catalyst loading of 5 g is even higher than 10 g. It might be influenced by both the concentration of produced epoxides and the production rate. A higher concentration of epoxides could let the ring-opening reaction obtain them easier.

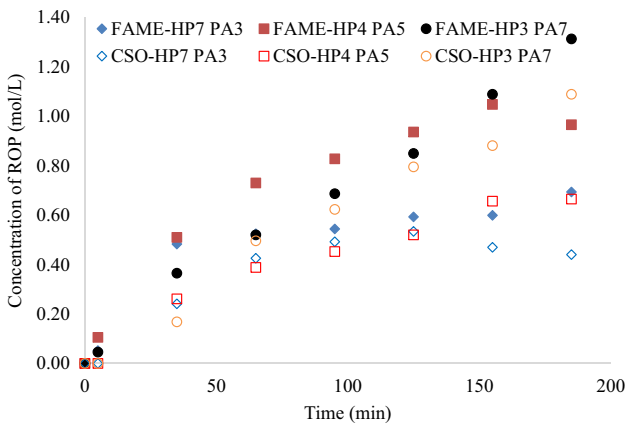

Fig. 10 Effects of HP/PA ratio on the ring-opening products

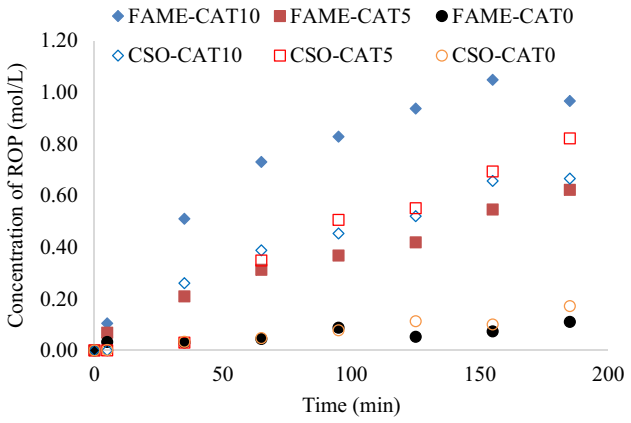

Fig. 11 Effects of catalyst loading on the ring-opening products

4 Conclusion

Functionalization of vegetable oil via epoxidation is vital in chemical industry, and the use of percarboxylic acids is the most common method. The drawback of this reaction system is the viscosity increase, side reaction of ring-opening, and risk of thermal runaway. To circumvent these drawbacks, vegetable oils were transesterified into FAME, solid acid catalyst was used, and perpropionic acid was used instead of performic acid.

A systematic comparison between the epoxidation of vegetable oil and FAME was done, which is missing in the literature. Cottonseed oil was used as raw materials and Amberlite IR-120 as a solid acid catalyst.

It was demonstrated that using perpropionic acid decreases the side reaction of ring-opening compared to performic acid.

After the transesterification, the methyl ester group was identified by FTIR and NMR spectra and GPC evidenced a decrease of the molecule weight. For the epoxidation of cottonseed oil (CSO) and fatty methyl ester of CSO (CSO-FAME), the oxirane ring signals could be found in both FTIR and NMR spectra, and a slight increase of molecule weight for the epoxides products was observed in GPC results.

The kinetics of epoxidation was compared between CSO, and CSO-FAME was explored. The results show that although the epoxidation reaction rate was rapid in CSO-FAME, the ring-opening reaction rate was faster in CSO-FAME by perpropionic acid. The oligomerization of the three-armed star structure of ECSO could allow a higher double-bound access compared to the linear oligomerization of ECSO-FAME. This steric difference could explain the higher production of epoxide during the epoxidation of CSO compared to CSO-FAME.

One should favor using CSO as starting material and a high HP/PA ratio to obtain a higher yield in the epoxide group.

Surprisingly, this paper shows that the kinetics of epoxidation by perpropionic acid is better for CSO than for CSO-FAME, where the unsaturated group is more accessible at the beginning of the reaction. A further investigation is needed, concerning the oligomerization mechanism for CSO and CSO-FAME.

Abbreviations CA: carboxylic acid; CSO: cottonseed oil; CSO-FAME: cottonseed oil fatty acid methyl ester; ECSO: epoxidized cottonseed oil; ECSO-FAME: epoxidized cottonseed oil fatty acid methyl ester; DB: double bond; EP: epoxidized group; FA: formic acid; PA: propionic acid; HP: hydrogen peroxide; CAT: catalyst; ROP: ring-opening products

Supplementary Information The online version contains supplementary material available at https://doi.org/10.1007/s13399-023-04985-1.

Acknowledgements This article is part of the ARBRE project. The China Scholarship Council: Cooperation Program with the UTs and INSAs (France) is thanked by the authors.

Author contribution Conceptualization, Y.M., N.K., and S.L.; methodology, Y.M., N.K., and S.L.; software, Y.M., N.K.; validation, Y.M.; writing (original draft preparation), Y.M., N.K., and S.L.; writing (review and editing), Y.M., N.K., and S.L.; supervision, N.K. and S.L.; funding acquisition, S.L. All authors have read and agreed to the published version of the manuscript.

Funding ARBRE is co-funded by the European Union through the European Regional Development Fund (ERDF, agreement n° 00130305) and by Normandy Region (agreement n° 21E05304), via the support of "pôle CTM (Continuum Terre-Mer) and EP2M (Energies, Propulsion, Matière, Matériaux) de Normandie université."

Data Availability The data that support the findings of this study are available from the corresponding author upon reasonable request.

Declarations

Ethical approval Not applicable.

Competing interests The authors declare no competing interests.

References

1. Williams CK, Hillmyer MA (2008) Polymers from renewable resources: a perspective for a special issue of polymer reviews. Polym Rev 48:1–10. https://doi.org/10.1080/15583720701834133
2. Adekunle KF (2015) A review of vegetable oil-based polymers: synthesis and applications. Open J Polym Chem 05:34–40. https://doi.org/10.4236/OJPCHEM.2015.53004
3. Gebremariam SN, Marchetti JM (2017) Biodiesel production technologies: review. AIMS Energy 5:425–457. https://doi.org/10.3934/ENERGY.2017.3.425
4. Mittal V, Talapatra KN, Ghosh UK (2022) A comprehensive review on biodiesel production from microalgae through nano-catalytic transesterification process: lifecycle assessment and methodologies. Int Nano Lett 12:351–378. https://doi.org/10.1007/S40089-022-00372-2

5. Murawski A, Quirino RL (2018) Vegetable oils as a chemical platform. In: Polymer gels. Springer, Singapore, pp 125–152
6. Lligadas G, Ronda JC, Galià M, Cádiz V (2013) Renewable polymeric materials from vegetable oils: a perspective. Mater Today 16:337–343. https://doi.org/10.1016/J.MATTOD.2013.08.016
7. Maisonneuve L, Lamarzelle O, Rix E et al (2015) Isocyanate-free routes to polyurethanes and poly(hydroxy urethane)s. Chem Rev 115:12407–12439. https://doi.org/10.1021/ACS.CHEMREV.5B00355
8. Benaniba MT, Belhaneche-Bensemra N, Gelbard G (2007) Kinetics of tungsten-catalyzed sunflower oil epoxidation studied by 1H NMR. Eur J Lipid Sci Technol 109:1186–1193. https://doi.org/10.1002/EJLT.200700114
9. Pérez-Sena WY, Cai X, Kebir N et al (2018) Aminolysis of cyclic-carbonate vegetable oils as a non-isocyanate route for the synthesis of polyurethane: a kinetic and thermal study. Chem Eng J 346:271–280. https://doi.org/10.1016/J.CEJ.2018.04.028
10. Mahadi MB, Azmi IS, Kadir MZA et al (2023) Sustainable epoxidation of expired palm oil–derived oleic acid via in situ peracid mechanism with applied ion resin Amberlite IR-120H: from waste to wealth. Biomass Convers Biorefin:1–9. https://doi.org/10.1007/s13399-023-04019-w
11. Wisniak J, Cancino A, Vega JC (1964) Epoxidation of anchovy oils. Ind Eng Chem Prod Res Dev 3:306–311. https://doi.org/10.1021/I360012A012
12. Wisniak J, Navarrete E (1970) Epoxidation of fish oil kinetic and optimization model. Ind Eng Chem Prod Res Dev 9:33–41. https://doi.org/10.1021/I360033A006
13. Azmi IS, Jalil MJ, Hadi A (2022) Epoxidation of unsaturated fatty acid–based palm oil via peracid mechanism as an intermediate product. Biomass Convers Biorefin:1–9. https://doi.org/10.1007/S13399-022-02862-X/METRICS
14. Maia DLH, Fernandes FAN (2022) Influence of carboxylic acid in the production of epoxidized soybean oil by conventional and ultrasound-assisted methods. Biomass Convers Biorefin 12:5861–5868. https://doi.org/10.1007/S13399-020-01130-0
15. Prileschajew N (1909) Oxydation ungesättigter Verbindungen mittels organischer Superoxyde. Ber Dtsch Chem Ges 42:4811–4815. https://doi.org/10.1002/CBER.190904204100
16. Leveneur S (2017) Thermal safety assessment through the concept of structure-reactivity: application to vegetable oil valorization. Org Process Res Dev 21:543–550. https://doi.org/10.1021/ACS.OPRD.6B00405
17. Musakka N, Salmi T, WärnÅ J et al (2006) Modelling of organic liquid-phase decomposition reactions through gas-phase product analysis: model systems and peracetic acid. Chem Eng Sci 61:6918–6928. https://doi.org/10.1016/J.CES.2006.07.033
18. Chen J, De Liedekerke BM, Gyurik L et al (2019) Highly efficient epoxidation of vegetable oils catalyzed by a manganese complex with hydrogen peroxide and acetic acid. Green Chem 21:2436–2447. https://doi.org/10.1039/C8GC03857K
19. Wu Z, Nie Y, Chen W et al (2016) Mass transfer and reaction kinetics of soybean oil epoxidation in a formic acid-autocatalyzed reaction system. Can J Chem Eng 94:1576–1582. https://doi.org/10.1002/CJCE.22526
20. Campanella A, Baltanás MA (2006) Degradation of the oxirane ring of epoxidized vegetable oils in liquid–liquid heterogeneous reaction systems. Chem Eng J 118:141–152. https://doi.org/10.1016/J.CEJ.2006.01.010
21. Campanella A, Baltanás MA (2007) Degradation of the oxirane ring of epoxidized vegetable oils in a liquid–liquid–solid heterogeneous reaction system. Chem Eng Process Process Intensif 46:210–221. https://doi.org/10.1016/J.CEP.2006.06.001
22. Leung DYC, Wu X, Leung MKH (2010) A review on biodiesel production using catalyzed transesterification. Appl Energy 87:1083–1095. https://doi.org/10.1016/J.APENERGY.2009.10.006
23. Fukuda H, Kondo A, Noda H (2001) Biodiesel fuel production by transesterification of oils. J Biosci Bioeng 92:405–416. https://doi.org/10.1016/S1389-1723(01)80288-7
24. Körbitz W (1999) Biodiesel production in Europe and North America, an encouraging prospect. Renew Energy 16:1078–1083. https://doi.org/10.1016/S0960-1481(98)00406-6
25. Cai X, Matos M, Leveneur S (2019) Structure-reactivity: comparison between the carbonation of epoxidized vegetable oils and the corresponding epoxidized fatty acid methyl ester. Ind Eng Chem Res 58:1548–1560. https://doi.org/10.1021/ACS.IECR.8B05510
26. Huang YB, Yao MY, Xin PP et al (2015) Influence of alkenyl structures on the epoxidation of unsaturated fatty acid methyl esters and vegetable oils. RSC Adv 5:74783–74789. https://doi.org/10.1039/c5ra11035a
27. Omonov TS, Kharraz E, Curtis JM (2016) The epoxidation of canola oil and its derivatives †. https://doi.org/10.1039/c6ra17732h
28. Azmi IS, Ozir TAZT, Rasib IM et al (2022) Synergistic epoxidation of palm oleic acid using a hybrid oxygen carrier solution. Biomass Convers Biorefinery. https://doi.org/10.1007/S13399-022-03325-Z
29. Leveneur S, Wärnå J, Salmi T et al (2009) Interaction of intrinsic kinetics and internal mass transfer in porous ion-exchange catalysts: green synthesis of peroxycarboxylic acids. Chem Eng Sci 64:4101–4114. https://doi.org/10.1016/J.CES.2009.05.055
30. Leveneur S, Thönes M, Hébert J-P et al (2012) From kinetic study to thermal safety assessment: application to peroxyformic acid synthesis. Ind Eng Chem Res 51:13999–14007. https://doi.org/10.1021/ie3017847
31. Campanella A, Fontanini C, Baltanás MA (2008) High yield epoxidation of fatty acid methyl esters with performic acid generated in situ. Chem Eng J 144:466–475. https://doi.org/10.1016/J.CEJ.2008.07.016
32. Leveneur S, Ledoux A, Estel L et al (2014) Epoxidation of vegetable oils under microwave irradiation. Chem Eng Res Des 92:1495–1502. https://doi.org/10.1016/J.CHERD.2014.04.010
33. Maerker G (1965) Determination of oxirane content of derivatives of fats. J Am Oil Chem Soc 42:329–332. https://doi.org/10.1007/BF02540140
34. Mungroo R, Goud VV, Pradhan NC, Dalai AK (2011) Modification of epoxidised canola oil. Asia-Pacific J Chem Eng 6:14–22. https://doi.org/10.1002/APJ.448
35. Rabelo SN, Ferraz VP, Oliveira LS, Franca AS (2015) FTIR Analysis for quantification of fatty acid methyl esters in biodiesel produced by microwave-assisted transesterification. Int J Environ Sci Dev 6:964–969. https://doi.org/10.7763/IJESD.2015.V6.730
36. Wai PT, Jiang P, Shen Y et al (2019) Catalytic developments in the epoxidation of vegetable oils and the analysis methods of epoxidized products. RSC Adv 9:38119–38136
37. Meng Y, Kebir N, Cai X, Leveneur S (2023) In-depth kinetic modeling and chemical analysis for the epoxidation of vegetable oils in a liquid–liquid–solid system. Catalysts 13:274. https://doi.org/10.3390/catal13020274